A decentralized radio network for small groups of unmanned aerial vehicles

Patryk SZYWALSKI and **Andrzej WAINDOK**[ID]*

Faculty of Electrical Engineering, Automatic Control and Informatics, Department of Electrical Engineering and Mechatronics,
Opole University of Technology, Opole, Poland

Abstract. The investigation of a decentralized radio network dedicated to unmanned aerial systems (UASs) was presented in the paper. Two frequencies (315 MHz; 434 MHz) and five different configurations of Gaussian frequency-shift keying (GFSK) were taken into account. Three different algorithms for decentralized networks were investigated and their influence on the network capacity was measured. The research was done both for static and dynamically changed unmanned aerial vehicle (UAV) positions. In order to quantify the research three different parameters were determined: RSSI, nP (number of data packets in one second), and F (frequency of data update).

Keywords: decentralized communication; unmanned aerial vehicles (UAVs); unmanned aerial system (UAS).

1. INTRODUCTION

The unstable geopolitical situation has led to a strong and constantly growing interest in unmanned systems. Unmanned aerial systems (UAS) are used in such fields as movie and aerial photography, geodesy, protection of people and property, inspections, assistance in assessing damage, providing access to the radio network, medical rescue, and delivery of parcels. UAVs also contribute to the development of other fields of science. There are applications in which UAVs collect data to study volcano tectonics and tectonic features in the active Icelandic rift [1]. It is also possible to use UAS to provide Internet connectivity in the area affected by the disaster [2]. UAVs have also been used during periodic, visual inspections of photovoltaic farms [3] or medical transports [4]. UAS implementations in agriculture are becoming increasingly common, as well. Advanced vision systems mounted on UAVs can detect the disease of pumpkin [5] or citrus plants [6], enabling earlier counteraction. Often UAVs are part of a large agricultural system, which, using artificial intelligence, based on the collected data, can make a detailed analysis, striving to maximize the efficiency of agriculture [7].

These devices are characterized by high maneuverability, low weight, and low production costs, and do not require human presence on board [8]. The operator controlling the movement of the device most often communicates with it by radio using dedicated equipment for this purpose. Currently, systems that operate automatically or autonomously are already possible. In this case, the operator can supervise the operation of the device, but the control unit on the device manages the movement. In order to increase efficiency, UAVs are combined into groups,

creating unmanned aerial systems (UASs) [9]. UAS is defined as a set of several cooperating UAVs combined into one system. The UAS includes flying devices - UAVs and the entire ground equipment. Some solutions allow mobile robots to recognize characteristic objects [10]. The universality and multitasking of the system can be ensured by decentralized control. This means that there is no hierarchy in the activities performed. The loss of one group member consequently does not affect the stability and success of the mission. Controlling a decentralized group of UAVs requires appropriate algorithms not only in terms of position control but also the structure of the radio network. It should ensure uninterrupted communication of all UAVs, regardless of any failures of individual units. The division of tasks (duties) within a resource-constrained UAS in an unfamiliar environment is still a challenging problem. Mainly due to limited information about a very dynamic environment, the lack of a continuous and reliable communication network, and limitations related to the available energy [11]. In traditional single-channel radio networks bandwidth is limited by radio capabilities, interference, and collisions [12].

The advantage of the local radio network is its encapsulation. The power of the transmitters can be adjusted to the maximum distance of the UAS operation, thus limiting the possibility of its detection or interference. An alternative system assumes the use of a mobile network. There has been a huge technological revolution in a few decades from first-generation (1G) technology with a data rate of Kbps to fifth-generation (5G) technology with a data rate of Gbps [13]. The prominent capacities of 5G New Radio (5G NR) cellular networking drive the rapid development of many fields. The ubiquitous implementations of 5G NR cellular networking also provide swarm unmanned aircraft system (UAS) networking with the feasibility of scalable deployment and smart control [14]. There are also hybrid solutions where each UAV connects to the base station using the cellular network, but communication in the UAS takes place using the local radio network [15].

*e-mail: a.waindok@po.edu.pl

In the field of UAV control, there are many publications based on the leader-follower relationship between the UAV in the UAS. This control makes one device directly dependent on another (leader), which makes it impossible to manage the network in a decentralized manner [16]. Therefore, the loss of one member in the network causes a disturbance in the hierarchy of the entire system [17]. The definition of decentralized UAS is possible when devices can operate autonomously at the level of position control [18] and radio network management, while guaranteeing operational stability. The novelty presented in the paper is an algorithm that is robust against disturbances in the UAS. In order to test the algorithm, the communication inside the radio network for small groups (up to five UAVs) of unmanned aerial devices was investigated. The tests were made for two different frequencies (315 MHz; 434 MHz) and five different configurations of Gaussian frequency-shift keying (GFSK). Three different algorithms for decentralized networks were tested.

A simple and cheap RFM69HC module was used for network communication. It operates on the 434 MHz band. According to the International Amateur Radio Union (IARU) findings, this frequency can be used for amateur purposes, including research [19]. The ethics of a scientist require not to broadcast/interfere with other bands used by government and civil institutions, even when conducting research. During the research, the UAS was extended with a Local Positioning System (LPS) by Marvelmind. The navigation system also used the 434 MHz bands. To avoid interference, the RFM69HC modules were tested on the 315 MHz band, as well. The transmitter power did not allow the wave to be detected outside the laboratory while guaranteeing that other users of this frequency would not be disturbed.

2. PRELIMINARY RESEARCH

Wireless radio networks consist of a group of nodes (users) interconnected by a wireless medium [20]. Sending information between nodes inevitably causes communication delays [21]. In many practical implementations, some unexpected and uncontrollable events can subsequently occur [22]. Current implementations typically use the RSSI (received signal strength indicator) as the decision-maker in routing. This often causes association errors with multiple radio signals and the well-known problem of the ping-pong effect [23]. The disadvantage of using the RSSI parameter is also its high dependence on environmental and weather conditions [24]. The first study was to determine the maximum stable radio transmission connection. Figure 1 shows the recorded RSSI for selected distances between the radio transmitter and receiver. The test was performed using the RFM69HC 434 MHz module and a quarter dipole antenna.

Initially, it was assumed that the system would be able to work with the use of a mesh library for generating mesh topology. It contains solutions enabling the transfer of information from one device to another, taking into account the optimal path for sent data packets. This library, based on the RSSI parameter, can determine the optimal route for information transfer. It is
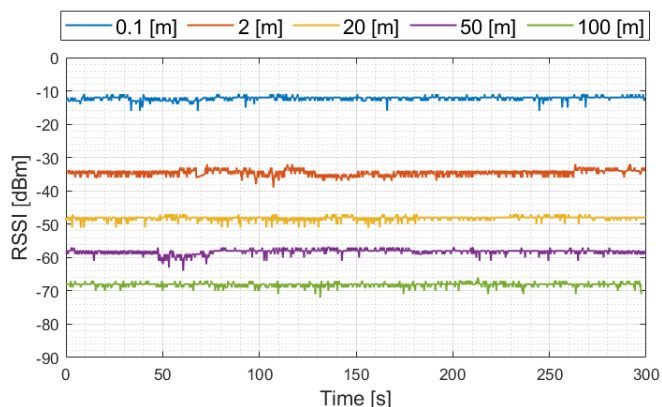
Fig. 1. Dependence of transmitter-receiver antenna distance on the RSSI parameter

also possible to use other users in the network as connectors to provide information [25].

Figure 2a shows an exemplary mesh network topology. The blue lines indicate a connection between two network users. The use of the solution facilitates sending a data packet between points $1 \leftrightarrow 5$, although there is no direct connection between them. This is its advantage. However, the tests showed some significant disadvantages. The first was the low frequency of information exchange, reaching a maximum of 2 Hz. The second disadvantage was errors caused by the inaccuracy of using the RSSI parameter as a decision-maker of the information route. At small distances, not exceeding 20 meters, this parameter was "excellent" in all options, according to Table 1.
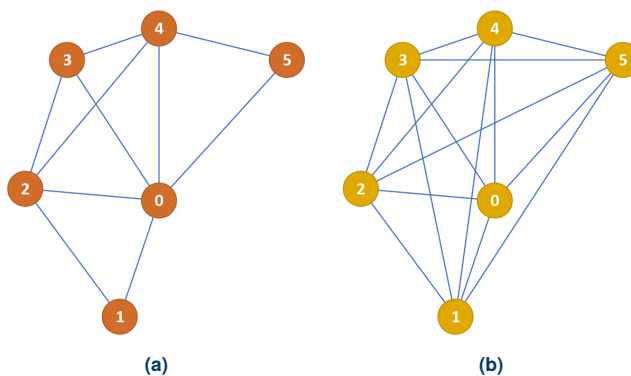
Fig. 2. Topology: (a) example for mesh library, (b) classic solution

Table 1
Classification of signal quality as a function of its power

Signal strength (dBm)	Classification
$-30 \div 0$	Excellent
$-67 \div -30$	Very good
$-70 \div -67$	Good
$-80 \div -70$	Bad
$-90 \div -80$	Very bad

2

Bull. Pol. Acad. Sci. Tech. Sci., vol. 72, no. 1, p. e147922, 2024

Although the devices could communicate directly, the information received in the tests was not always provided directly. Problems arise during the movement of devices, which the routing could not keep up with. The use of the mesh solution does not allow for sufficient speed in the network. The movement of an unmanned aerial vehicle causes large vibrations. In such conditions, the RSSI parameter is not stable enough to determine the route of data packet transmission on its basis. These problems were also noticed by the author of the library, who finally recommends using the solution only for static devices with a frequency of up to 1 Hz.

The RFM69HC radio communication module used in the project could be reprogrammed to a different carrier frequency. This solution is convenient because sometimes other systems, also operating on the 434 MHz band, may interfere with each other. As part of the tests, the module was also verified for the carrier frequency of 315 MHz. Another research goal was to select a modulation that would guarantee the highest possible frequency of data packet transmission with the lowest possible bandwidth. The use of a wide band in radio communication allows for easier detection, interception, and disruption of the network [26]. In addition, the network itself may interfere with other receivers operating on the 434 MHz band, including garage doors, car remote controls, etc. In Table 2 types of radio modulation used in the project were given.

Table 2
Modulation types

	Modulation	Parameters	
1.	GFSK_Rb19_2Fd38_4	Rb = 19.2 kbs,	Fd = 38.4 kHz
2.	GFSK_Rb38_4Fd76_8	Rb = 38.4 kbs,	Fd = 76.8 kHz
3.	GFSK_Rb57_6Fd120	Rb = 57.6 kbs,	Fd = 120 kHz
4.	GFSK_Rb125Fd125	Rb = 125 kbs,	Fd = 125 kHz
5.	GFSK_Rb250Fd250	Rb = 250 kbs,	Fd = 250 kHz

As part of the research, the spectral verification of the radio signal was conducted for the frequencies of 434 MHz and 315 MHz. In Fig. 3 the radio wave spectrum recorded by the signal analyzer is shown. According to the recommendations of the producer of the RFM69HC module, the RadioHead library was used, which allows for OOK (on-off keying), FSK (frequency-shift keying) and GFSK (Gaussian frequency-shift keying) modulation. During all the tests conducted for this article, GFSK modulation was used in various configurations, as potentially the most resistant to external disturbances. GFSK is an extension of the FSK modulation scheme, where the frequency of the modulated signal is not instantaneously changed at the beginning of each symbol period of the binary data.

It was initially assumed that the data exchange in the network should be at least 20 Hz for five UAVs. The minimum network bandwidth had to be 19.2 kbs (theoretically obtaining 24.57 Hz) [27]. Lower frequencies could lead to in-flight UAV collisions due to the lack of sufficient knowledge of the position of other members of the network. It was expected, however, that

(a)

(b)
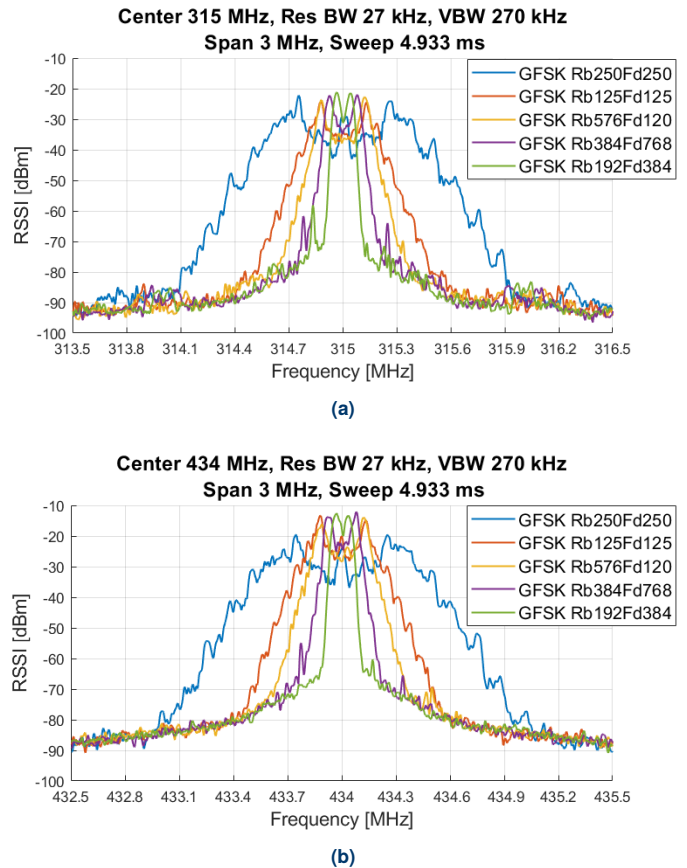
Fig. 3. Signal analyzer indications of selected wave modulations: (a) 315 MHz, (b) 434 MHz

during the tests, the results may differ from those under ideal conditions, in addition to only two network users. Therefore, it was decided to investigate modulations that occupy a larger band than originally assumed.

Based on the results presented in Fig. 3, it can be concluded that the module works correctly for all modulations and two carrier frequencies. The only negative aspect is the deterioration of the RSSI factor for 315 MHz (compared to 434 MHz). The results of the RSSI parameter measurements, depending on the modulation, are presented in Table 3.

Table 3
RSSI values for different modulation types

Frequency [MHz]	Channel power depending on the modulation [dBm]				
	1	2	3	4	5
315	–21.39	–20.82	–23.64	–23.59	–26.56
434	–6.88	–7.94	–7.3	–8.33	–9.66

The presented results were obtained using UAVs. Figures 4 and 5 show RSSI for three cases of UAS radio network configuration. Analysis of Fig. 4. shows that if the transmitting and receiving modules are stationary, the RSSI parameter changes its value by a maximum of 2 dBm (434 MHz). This deviation

Bull. Pol. Acad. Sci. Tech. Sci., vol. 72, no. 1, p. e147922, 2024

3

is consistent with the principle of operation of radio networks and should not affect data transmission under normal conditions. If one of the modules makes a move, the RSSI parameter changes very quickly, causing routing errors. Figure 5 shows the same test in terms of transmission parameters, transmitter, and receiver positions, but the device was in an overhang. Discrepancies of up to 30 dBm in the RSSI parameter were recorded. This led to a distortion of the routing, which resulted in sending a data packet in a roundabout way. A delay in the delivery of certain data packets was also noticed, i.e. the data sent from the same transmitting module arrives later than the previously sent information.
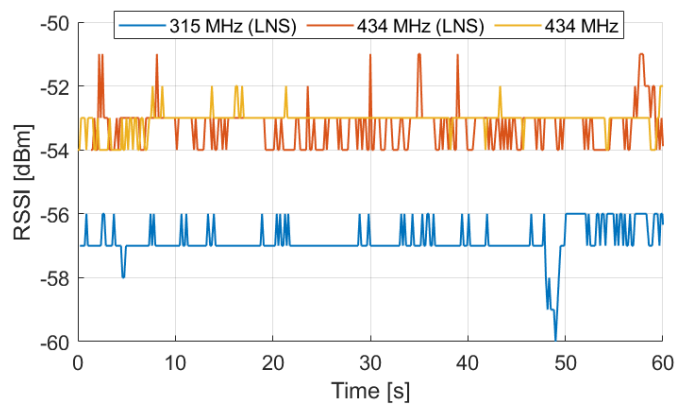
Fig. 4. Static characteristics of different network configurations
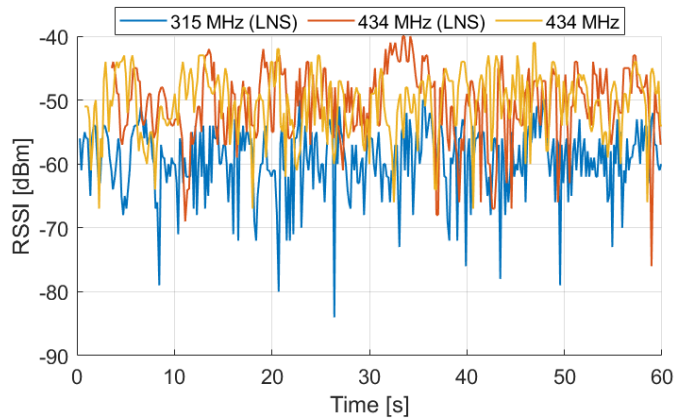
Fig. 5. Dynamic characteristics of different network configurations – overhang at a height of 2 meters

In Table 4 the calculated average values of the RSSI parameter from the tests were given. It was also tested whether the Marvelmind local navigation system (LNS), also using communication on the 434 MHz band, does not interfere with network communication. Based on the tests, no deterioration of the radio network performance was registered. The use of the carrier frequency of 434 MHz led to the disconnection of the navigation modules, deteriorating its positioning properties. For the frequency 315 MHz, compared to the 434 MHz, 3 dBm deterioration of the RSSI parameter for static and 9 dBm for dynamic tests was observed. Based on the tests, it was found that both the navigation system and the radio network, despite the worse

RSSI parameter, in the 315 MHz configuration work stably. According to the signal classification in Table 1, the transmission quality during the flight, even for the least favorable 315 MHz (LNS) configuration, is very good. However, such a solution shortens the maximum range of the radio modules.

Table 4
Average RSSI value for different UAS configurations

Configuration	RSSI [dBm]	
	Static tests	Overhang at a height of 2 m
315 MHz (LNS)	−56.85	−59.36
435 MHz (LNS)	−53.27	−50.64
434 MHz	−53.02	−50.59

3. ASSUMPTIONS OF THE RADIO NETWORK

Combining many UAVs into one system required the formulation of several basic assumptions. Each device in the network has a permanent, individual identification number. Numbering from 0 to n_{max} (maximum number of users in the network) was adopted, where 0 was assigned to the operator panel, and values bigger than zero to UAVs. The identification number for a given device is always the same, also in the description of navigation systems, control systems, construction, or annotation on the control panel and is located on the casing of each device. The structure of the network resembles the mesh topology shown in Fig. 2b. It is therefore assumed that each device has a direct connection to every other device.

One of the main research goals was to make the reactions of one member of the network independent of the other, despite their direct connections. Contrary to the classic leader-follower strategy, the proposed algorithm of information exchange within the network should work stably, regardless of temporary changes in the number of network members. By stating the stability of the network operation, we mean its resistance to factors, most often random and negatively affecting the entire group. Such action may be the loss of one network member, which is also a node through which information is transmitted, or the frequent entry/exit of a network member when the device is at the edge of the radio communication range.

The network operation structure was designed based on the following assumptions:

- Network users connect directly, dynamically, and non-hierarchically.
- A new user can enter the network and leave it in a way that does not threaten the stability of information exchange between other users.
- The maximum number of users is fixed and declared at system startup.
- The number of members in the network can change dynamically.
- Data transmission is encrypted, and access to the network is possible only with the knowledge of a 16-byte key.

4

Bull. Pol. Acad. Sci. Tech. Sci., vol. 72, no. 1, p. e147922, 2024

- A break in data transmission longer than one second is unacceptable.
- Each module working within the network must have observer or network member status.

Within the network, users have two states. A member (or alternatively named user) of the network can both receive and send packets of data. This status is reserved for UAVs. Due to the character of this work, the operator panel also has this status, which is needed to send appropriate instructions, e.g. in emergency situations.

The observer does not directly participate in the exchange of data packets within the network – they can only listen to it in order to collect data. This status is reserved for the module responsible only for visualizations of UAS work. Given the fact that this module does not introduce any information into the network, no member has to wait for their data package. Based on research, the presence of the observer does not reduce the frequency of data packet exchange within the network. An infinite number of network observers is therefore possible.

A data packet is understood as a set of parameters sent once in the form of one piece of information. As part of the research, the behavior of the network for a data packet size of 20 Bytes was examined. During the research, the data packet has a fixed size and is known by each device. In this way, it is easy to verify whether information has been distorted.

An important issue is the loss of data packets during transmission or its distortion. Each UAV receiving data checked the CRC of the entire data packet and assessed the reliability of each parameter. For example, the magnetometer reading could not be bigger than 360 and less than 0, the position could not change by more than the maximum speed of the UAV, etc. Each UAV in a given sequence waits up to 50 ms for a data packet from the user to whom the given sequence belongs. Failure to collect 20 consecutive data packets from one member caused them to be considered absent from the network and led to reduced n_{max}.

4. WORKING PRINCIPLE

In Fig. 6 the block diagram of the radio network was presented. Each device after the start creates the following variables:
- Sequence number: SEQ = 1.
- Loop iteration: $i = 1$.
- Dynamic table in which the presence of the UAV in the selected iteration is registered.

The number of DynTab rows depends on the maximum number of network members. The number of columns reflects the delay of the network reaction to a possible loss of communication with any user. The research refers to nine network users (eight UAVs + one for the operator panel) ×20. The parameters are created by each network user individually and may differ at certain stages of the system operation. In order to achieve the main assumption, which is the decentralization of the radio network, each transmitter sent a packet of data simultaneously to many receivers, without waiting for acknowledgment of receipt. As a result, the transmitter does not have direct access to information on the number of receivers. Indirectly, the system will determine this number based on data packets received from
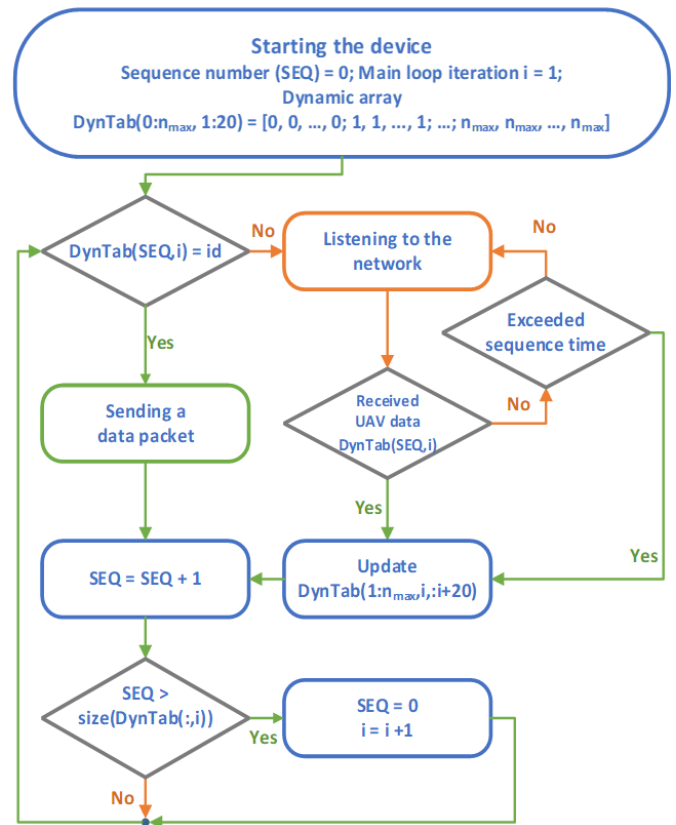
Fig. 6. Block diagram of communication within the radio network

other members of the network. On this basis, a list of active network users is created inside the device.

Each device checks if the value of DynTab(SEQ, i) matches the individual device number. If so, the device proceeds to the procedure of sending its data packet. Similarly, other users are listening to the network at the same time. The device, after sending its data packet, increments the sequence number and again compares the value of DynTab(SEQ, i) with its id.

As part of the research, three algorithms managing the network size were tested. In the first algorithm, a fixed, predefined size of the network was assumed. In the second algorithm, a dynamic resizing of the network was adopted, adding one additional sequence to the network listening to allow new users to enter quickly. The third algorithm did not have an additional listening sequence (compared to the second algorithm), because it was assumed that the modules would receive a data packet (of a new member) replacing the information of another member already in the network in one sequence. The network, detecting such an anomaly, increases its own.

5. RADIO NETWORK TESTS

All tests were conducted in an original UAV laboratory developed by one of the authors (Patryk Szywalski). It is a room with dimensions $11 \times 15 \times 5$ meters equipped with the LPS (Marvelmind system). There were no obstacles in the room (similar to the open space).

P. Szywalski and A. Waindok

5.1. Static tests

Static tests assumed the transmission of 20 Bytes in the 315 MHz and 434 MHz radio networks. The results for the first algorithm, i.e. a fixed network size of 434 MHz, are presented in Table 5. The measurements indicated the same frequency of receiving the data packet for both tested frequencies, however, for 315 MHz the signal power factor was weaker by 5–6 dBm. The nP parameter represents the number of packages received ($10 \times$ uint16_t) by the module placed in the central part of the circle (the other 8 are placed at equal distances from the circle with a diameter of 10 m). The F parameter represents the actual update frequency of the data packet from each member in the network. The tests in Table 5 were performed for five different modulations. According to Table 1 starting from one to five modulations, the bandwidth of data transmission was increased, obtaining successively greater network capacity. The network at the maximum size (nine members) and for the fifth modulation

Table 5
Measurements for the $10 \times$ uint16_t data package

Network size	Parameters	1.GFSK_Rb 19_2Fd38_4	2.GFSK_Rb 38_4Fd76_8	3.GFSK_Rb 57_6Fd120	4.GFSK_Rb 125Fd125	5.GFSK_Rb 250Fd250
2	nP	25.8	47.2	64.8	109.5	147.4
	F	25.8	47.2	64.8	109.5	147.4
	RSSI	−57.2	−56.6	−58.8	−56.2	−56.6
3	nP	34.5	63.1	87.6	148.2	207.7
	F	17.25	31.55	43	74.1	103.85
	RSSI	−65.1	−64.2	−66.1	−63.7	−62.8
4	nP	38.8	71.3	96.2	165.6	233.5
	F	12.9	23.8	32	55.2	77.8
	RSSI	−59.5	−60.4	−62.4	−59.7	−59.1
5	nP	41.5	75.1	102.8	173.6	250.4
	F	10.375	18.775	25.7	43.4	62.6
	RSSI	−58.2	−58.9	−60.9	−31.4	−58
6	nP	43.1	78.8	109.3	181.6	260.6
	F	8.6	15.8	21.9	36.3	52.1
	RSSI	−58.5	−57.6	−59.7	−56.4	−57.2
7	nP	44.4	81.4	110.4	191	273.8
	F	7.4	13.6	18.4	31.8	45.6
	RSSI	−57	−56.3	−58.3	−55.1	−55.3
8	nP	45.7	84	111.5	200.4	287.2
	F	6.5	12	15.93	28.6	41
	RSSI	−55.6	55.1	−56.9	−54.2	−54.1
9	nP	46.5	83.6	119.1	205.6	298.9
	F	5.8125	10.45	14.8875	25.7	37.3625
	RSSI	−52.9	−52.3	−54.2	−51.3	−51.6

worked stably, reaching the frequency of 37 Hz. Based on the results, it was decided to use modulation 3 during flights, i.e. GFSK_Rb57_6Fd120.

The next step was to test the behavior of the network for its dynamically changing size (algorithms 2 and 3). Comparing both solutions with the classical approach (algorithm 1, when $n_{\max}$ = const), no significant decrease in the frequency vs. number of users is observed (Table 6). The results indicate the correct operation of both algorithms that dynamically change the network size. Algorithm 3 was characterized by a longer network stabilization time (3 s) compared to algorithm 2 (500 ms).

Table 6
The frequency of updating the data packet (for GFSK_Rb57_6Fd120 modulation) of each member in the network, depending on the algorithm used

Algorithm		$n_{\max}$	Number of users in the network				
			$n = 2$	$n = 3$	$n = 4$	$n = 5$	$n = 6$
1	Constants network size n_{max} = const	2	65	–	–	–	–
		3	44	43	–	–	–
		4	40	27.5	32	–	–
		5	38	23.5	21.7	26	–
		6	36	22	18.3	18	22
2	Dynamic network size	$n + 1$	44	27.5	21.7	18	22
3		n	65	43	32	26	22

6. DYNAMIC TESTS – CIRCLE FLIGHT

In Fig. 7 the RSSI parameter recorded on each device during the circle flight (UAV → control panel) was presented. All devices worked stably throughout the flight. There were no unplanned disconnections or removals from the network during the measurements.
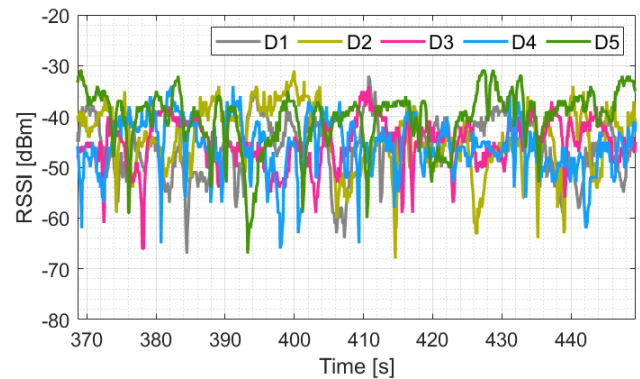
Fig. 7. RSSI parameter for five UAVs in flight on a circle

In Fig. 8 frequency values for data packets exchanging between devices during the flight (in a circle with 6 m diameter) of all five UAVs and one receiving panel were shown. Tests conducted for modulation GFSK_Rb57_6Fd120 indicate that a stable frequency of 20–22 Hz for exchanging data packets in

6

Bull. Pol. Acad. Sci. Tech. Sci., vol. 72, no. 1, p. e147922, 2024
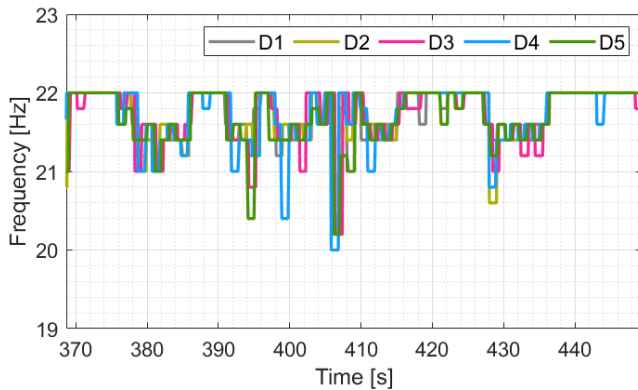
Fig. 8. The frequency of exchanging data packets between each UAV

the network was achieved. The discrepancy of 2 Hz is due to the fact that the transmission time depends on the distance, the position of the antenna, and the RSSI parameter. These parameters are not constant. Reducing the frequency of receiving data from the network on one device also reduces it on all other members in the network.

7. CONCLUSIONS

Based on the research published in the article, the following conclusions can be drawn:

- The proposed second and third algorithms meet the network decentralization condition allowing for a stable, non-hierarchical, and dynamic network size change.
- The used RFM69HC module has a 434 MHz carrier wave. For the 315 MHz frequency, an average of 5–6 dBm worse signal strength was recorded at a distance of five meters, which has a direct impact on the network coverage.
- Increasing the bandwidth of the wave increases the capacity of the network, but also its susceptibility to interference.
- The frequency of data transmission for each of the modulations decreases exponentially vs. the number of UAVs. Determining the maximum size of the network requires further research.
- No undesirable network activity was observed.

REFERENCES

[1] F.L. Bonali *et al.*, "UAV-based surveying in volcano-tectonics: An example from the Iceland rift", *J. Struct. Geol. of Structural Geology*, vol. 121, pp. 46–64, 2019, doi: 10.1016/j.jsg.2019.02.004.

[2] G. Choudhary, V. Sharma, and I. You, "Sustainable and secure trajectories for the military Internet of Drones (IoD) through an efficient Medium Access Control (MAC) protocol", *Comput. Electr. Eng.*, vol. 74, pp. 59–73, 2019, doi: 10.1016/j.compeleceng.2019.01.007.

[3] M.K. Nallapaneni, K. Sudhakar, M. Samykano, and V. Jayaseelan, "On the technologies empowering drones for intelligent monitoring of solar photovoltaic power plants", presented at the International Conference on Robotics and Smart Manufacturing (RoSMa2018), *Procedia Comput. Sci.*, vol. 133, pp. 585–593, 2018, doi: 10.1016/j.procs.2018.07.087.

[4] A. Pulvera and R. Weib, "Optimizing the spatial location of medical drones", *Appl. Geogr.*, vol. 90, pp. 9–16, 2018, doi: 10.1016/j.apgeog.2017.11.009.

[5] J. Abdulridha, Y. Ampatzidis, P. Roberts, and S.Ch. Kakarla, "Detecting powdery mildew disease in squash at different stages using UAV-based hyperspectral imaging and artificial intelligence", *Biosyst. Eng.*, vol. 197, pp. 135–148, 2020, doi: 10.1016/j.biosystemseng.2020.07.001.

[6] Y. Ampatzidis, V. Partel, B. Meyering, and U. Albrecht, "Citrus rootstock evaluation utilizing UAV-based remote sensing and artificial intelligence", *Comput. Electron. Agric.*, vol. 164, 104900, 2019, doi: 10.1016/j.compag.2019.104900.

[7] Y. Ampatzidis, V. Partel, and L. Costa, "Agroview: Cloud-based application to process, analyze and visualize UAV-collected data for precision agriculture applications utilizing artificial intelligence", *Comput. Electron. Agric.*, vol. 174, p. 105457, 2020, doi: 10.1016/j.compag.2020.105457.

[8] W. Zhang, M.W. Mueller, and R. D'Andrea, "Design, modeling and control of a flying vehicle with a single moving part that can be positioned anywhere in space", *Mechatronics*, vol. 61, pp. 117–130, 2019, doi: 10.1016/j.mechatronics.2019.06.004.

[9] Z. Zhen, G. Tao, Y. Xu, and G. Song, "Multivariable adaptive control based consensus flight control system for UAVs formation", *Aerosp. Sci. Technol.*, vol. 93, p. 105336, 2019, doi: 10.1016/j.ast.2019.105336.

[10] M. Podpora, A. Kawala-Sterniuk, V. Kovalchuk, G. Bialic, and P. Piekielny, "A distributed cognitive approach in cybernetic modelling of human vision in a robotic swarm", *Bio-Algorithms Med-Syst.*, vol. 16, no. 3, p. 20200025, 2020, doi: 10.1515/bams-2020-0025.

[11] S. Mousavi, F. Afghah, J.D. Ashdown, and K. Turck, "Use of a quantum genetic algorithm for coalition formation in large-scale UAV networks", *Ad Hoc Netw.*, vol. 87, pp. 26–36, 2019, doi: 10.1016/j.adhoc.2018.11.008.

[12] Y. Wu and M. Cardei, "Multi-channel and cognitive radio approaches for wireless sensor networks", *Comput. Commun.*, vol. 94, pp. 30–45, 2016, doi: 10.1016/j.comcom.2016.08.010.

[13] R. Shahzadi, M. Ali, H.Z. Khan, and M. Naeem, "UAV assisted 5G and beyond wireless networks: A survey", *J. Netw. Comput. Appl.*, vol. 189, p. 103114, 2021, doi: 10.1016/j.jnca.2021.103114.

[14] J. Wang, Y. Liu, S. Niu, and H. Song, "Lightweight blockchain assisted secure routing of swarm UAS networking", *Comput. Commun.*, vol. 165, pp. 131–140, 2021, doi: 10.1016/j.comcom.2020.11.008.

[15] D. Mishra, A. Trotta, E. Traversi, M. Di Felice, and E. Natalizio, "Cooperative Cellular UAV-to-Everything (C-U2X) communication based on 5G sidelink for UAV swarms", *Comput. Commun.*, vol. 192, pp. 173–184, 2022, doi: 10.1016/j.comcom.2022.06.001.

[16] C. Kownacki and L. Ambroziak, "Local and asymmetrical potential field approach to leader tracking problem in rigid formations of fixed-wing UAVs", *Aerosp. Sci. Technol.*, vol. 68, pp. 465–474, 2017, doi: 10.1016/j.ast.2017.05.040.

[17] R. Wang, M. Lungu, Z. Zhou, X. Zhu, Y. Ding, and Q. Zhao, "Least global position information based control of fixed-wing UAVs formation flight: Flight tests and experimental validation", *Aerosp. Sci. Technol.*, vol. 140, p. 108473, 2023, doi: 10.1016/j.ast.2023.108473.

[18] L. Ambroziak and Z. Gosiewski, "Two stage switching control for autonomous formation flight of Unmanned Aerial Vehicles", *Aerosp. Sci. Technol.*, vol. 46, pp. 221–226, 2015, doi: 10.1016/j.ast.2015.07.015.

[19] Krajowa Tablica Przeznaczeń Częstotliwości, Dz.U.2022.1988 t.j. https://isap.sejm.gov.pl/isap.nsf/DocDetails.xsp?id=WDU20 220001988

[20] K. Sohrabi, J. Gao, V. Ailawadhi, and G.J. Pottie, "Protocols for self-organization of a wireless sensor network", *IEEE Pers. Commun.*, vol. 7, no. 5, pp. 16–27, 2000, doi: 10.1109/98.878532.

[21] S. Shu and F. Lin, "Decentralized control of networked discrete event systems with communication delays", *Automatica*, vol. 50, no. 8, pp. 2108–2112, 2014, doi: 10.1016/j.automatica. 2014.05.035.

[22] S.J. Park, and K.H. Cho, "Decentralized supervisory control of discrete event systems with communication delays based on conjunctive and permissive decision structures", *Automatica*, vol. 43, no. 4, pp. 738–743, 2007, doi: 10.1016/j.automatica. 2006.10.016.

[23] H.D. Balbi, D. Passos, J. Vieira, C. Ricardo, L.C.S. Magalhães, and C. Albuquerque, "Towards a fast and stable filter for RSSI-based handoff algorithms in dense indoor WLANs", *Comput. Commun.*, vol. 183, pp. 19–32, 2022, doi: 10.1016/j.comcom. 2021.10.024.

[24] J. Luomala and I. Hakala, "Analysis and evaluation of adaptive RSSI-based ranging in outdoor wireless sensor networks", *Ad Hoc Netw.*, vol. 87, pp. 100–112, 2019, doi: 10.1016/j.adhoc. 2018.10.004.

[25] "RHMesh Class Reference," *RadioHead*. [Online]. Available: https://www.airspayce.com/mikem/arduino/RadioHead/classRH Mesh.html#details [Accessed: 20. June 2023].

[26] X. Zhang, T. Li, P. Gong, R. Liu, and X. Zha, "Modulation Recognition of Communication Signals Based on Multimodal Feature Fusion", *Sensors*, vol. 22, p. 6539, 2022, doi: 10.3390/s22176539.

[27] "RH_RF69 Class Reference," *RadioHead*. [Online]. Available: https://www.airspayce.com/mikem/arduino/RadioHead/class RH__RF69.html [Accessed: 20. June 2023].

8

Bull. Pol. Acad. Sci. Tech. Sci., vol. 72, no. 1, p. e147922, 2024